*Aust. J. Phys.*, 1980, **33**, 495–504

# A Comparison of Spectroscopic Models of Low Excitation $2^+$ States in $^{24}Mg$ and $^{28}Si$ from Inelastic Proton Scattering*

*K. Amos*,[A] *P. Nesci*[A] *and I. Morrison*[B]

[A] School of Physics, University of Melbourne, Parkville, Vic. 3052.
[B] Department of Theoretical Physics, Research School of Physical Sciences, Australian National University; present address: School of Physics, University of Melbourne.

*Abstract*

Distorted wave approximation analyses of the inelastic scattering of 49·5 MeV protons from $^{24}Mg$ and $^{28}Si$ are used to compare $2^+$ transition densities that were obtained from a standard shell model, deformed potential models and an $SU(3)$ model of the low excitation spectroscopy of these nuclei. Analysing power predictions do not reproduce the data adequately, and the discrepancies indicate a deficiency in the prescription for the transition mechanism.

## 1. Introduction

In a previous publication (Nesci *et al.* 1979), we used inelastic proton scattering data from $^{24}Mg$ and $^{28}Si$ to compare the single-particle transition densities associated with s–d basis shell and $SU(3)$ models of the spectroscopy of these nuclei. In that study the unnatural parity transitions (to the $3^+$ states) were considered primarily because the analyses should have been free of core polarization effects. The results of the study were at best inconclusive, and thus we now report on more extensive analyses of the $2_1^+$ state excitations for which model spectroscopies other than those of the shell and $SU(3)$ models can be used. Furthermore, for such transitions, the very sensitive analysing power data have been measured. We also present results of analyses of data from the excitation of the $2_2^+$ state in $^{24}Mg$, since our earlier analyses (Nesci *et al.* 1979) of data from the excitation of the $3_1^+$ state (supposedly also a $K = 2$ band state) revealed striking differences not only with the data but also between the model results themselves.

## 2. Model Spectroscopies

In the present study, conventional, *j–j* coupled, s–d shell model calculations of nuclear structure are used in distorted wave approximation (DWA) analyses of inelastic proton scattering data from $^{24}Mg$ and $^{28}Si$ as standards against which we can test analyses of the same data but with transition densities obtained from other models of the spectroscopy of these nuclei. The shell model calculations (of the structure and transition densities) of $^{24}Mg$ and $^{28}Si$ reported herein were made using the Chung and Wildenthal (1978) matrix elements with the Glasgow shell model program (Whitehead *et al.* 1977). In the case of $^{24}Mg$, it was feasible to use the full s–d shell basis space. Computational limitations, however, precluded us from doing so in the $^{28}Si$ case and necessitated limitations being made upon the occupancies of

* Research supported by a grant from the Australian Research Grants Committee.

the $d_{5/2}$ and $d_{3/2}$ orbits, as was the case in an earlier study (Wildenthal and McGrory 1973), such that the multiparticle basis had some 3000 states. As a direct consequence, the low excitation spectral properties of $^{24}$Mg and $^{28}$Si resulting from our analyses are in very good agreement with those of Wildenthal and McGrory, and require the usual shell model polarization charge of $0{\cdot}5\,e$ to reproduce the observed $\gamma$-ray transition rate from the ground state decay of the $2_1^+$ state in $^{24}$Mg. A larger value of $0{\cdot}63\,e$ is required to match the same decay in $^{28}$Si and the increase reflects, in part at least, the truncation of the full s–d basis space.

The $SU(3)$ model predictions are approximations to those of a full-basis shell model study, but the $SU(3)$ approach has the benefits of not only being elegant and simple, but also of emphasizing collectivity. Furthermore, whenever shell model studies can only be made using a truncated basis (as in our case for $^{28}$Si) the $SU(3)$ scheme provides an alternative spectroscopy from which one might discern other than gross effects of that truncation of the shell model basis. Whatever the circumstances, therefore, the $SU(3)$ model complements the shell model. Herein, we use the simplest plausible $SU(3)$ scheme to describe the ground and $2^+$ states in both nuclei, namely that all states can be obtained from single $SU(3)$ representations. Specifically we assume that the $0_1^+$, $2_1^+$ and $2_2^+$ states in $^{24}$Mg in which we are interested can all be derived from the $(8,4)$ $SU(3)$ representation, the first two states being members of the $K = 0$ band* with $2_2^+$ being the band head of the $K = 2$ band. This single representation model, and the choice of the $(8,4)$ case in particular, has been used with some success (Akiyama *et al.* 1969; Strottman 1972) albeit that the $2_2^+$ is known to occur at too low an excitation energy. We retain it nevertheless, not only because of its simplicity but also to enable a comparison of the results discussed herein with those of the $3^+$ state excitation reported previously (Nesci *et al.* 1979).

For $^{28}$Si we assume that the $0_1^+$ and $2_1^+$ states we require for the reaction studies are members of the $K = 0$ ground state band that can be deduced from the $(0,12)$ $SU(3)$ representation. This choice is consistent with an oblate minimal energy ground state, as has been obtained by Hartree–Fock calculations, which by using the Chung–Wildenthal (1978) matrix elements gives an oblate–prolate splitting of 6 MeV. This choice of an oblate solution is also consistent with the recently measured (Schwalm *et al.* 1977) large positive static quadrupole moment of the $2_1^+$ state in $^{28}$Si. As with the shell model prescriptions, the $SU(3)$ model spectroscopies require polarization charges to match the observed $B$(E2) values for the ground state electromagnetic decays of the $2_1^+$ states. These polarization charges are $0{\cdot}4\,e$ and $0{\cdot}21\,e$ for the $^{24}$Mg and $^{28}$Si cases respectively.

Ostensibly the polarization charges required by both shell and $SU(3)$ schemes are due to truncation to just the full s–d shell space at most. The projected Hartree–Fock (PHF) method permits realistic estimation of intrinsic structure of certain states in nuclei in terms of a much larger basis space. Indeed the ground state bands of $^{24}$Mg and $^{28}$Si can be represented by the appropriate projections from the single minimum energy determinant of an axially symmetric Hartree–Fock field. We will use such a large basis (0s–0g single-particle oscillator states) in a Hartree–Fock calculation (Braley and Ford 1969; Ford *et al.* 1971) for the ground state band in $^{24}$Mg. By so doing, the predicted $B$(E2) value for the de-excitation of the $2_1^+$ state matches the empirical one and no polarization charge is required.

* The $SU(3)$ model index $K$ is the orthogonal index (Draayer and Akiyama 1973) that distinguishes between multiple occurrences of total (orbital) angular momentum.

For the $0_1^+$ and $2_1^+$ states in $^{28}$Si, we have used results from an s–d shell basis PHF calculation, not only to resolve the numerical problems of the reaction calculations but also to provide an alternative viewpoint (in the s–d basis) of this nucleus. The importance of the relative role of this PHF calculation with respect to the $SU(3)$ and $j$–$j$ shell models is discussed in Section 3 below. Of course, with this PHF state a polarization charge, of $0{\cdot}32\,e$, is still necessary to match the observed $B$(E2) value, and so we have also used the Nilsson model to specify an appropriate deformed-basis single determinant from which the $0_1^+$ and $2_1^+$ states are obtained by projection and from which the empirical $B$(E2) value can be obtained with no polarization charge. The appropriate Nilsson field has quadrupole and hexadecapole deformations characterized by values of $\beta_2$ and $\beta_4$ of $-0{\cdot}21$ and $0{\cdot}05$ respectively. It should be noted that we constrained the variation so that $\beta_2$ would lie in the oblate region of values near $-0{\cdot}2$.

## 3. Details of Analyses

All the above described spectroscopies have been used in DWA analyses of the inelastic scattering of 49·5 MeV protons leading to the $2_1^+$ (1·37 MeV) and $2_2^+$ (4·24 MeV) states in $^{24}$Mg and of 49·5 MeV protons exciting the $2_1^+$ (1·78 MeV) state in $^{28}$Si. The reaction data used (Craig *et al.* 1966; Lewis *et al.* 1967; Rush *et al.* 1967) include analysing powers from the excitations of the $2_1^+$ states (projectile energies of 49·2 and 49 MeV for $^{24}$Mg and $^{28}$Si respectively). We use an anti-symmetrized microscopic DWA method of analysis (Geramb *et al.* 1975) in which data predictions relate to scattering amplitudes that have the form

$$T_{\mathrm{if}} = \sum_{j_1 j_2 I x} S^{(x)}(j_1 j_2; J_\mathrm{i} J_\mathrm{f}; I)\, M^{(x)}_{j_1 j_2 I}. \tag{1}$$

Here the spectroscopic amplitudes $S^{(x)}$ carry all the multiparticle information about the nuclear transition. With the superscript $x$ denoting protons and neutrons by $\pi$ and $\nu$ respectively, the spectroscopic amplitudes are defined by (Amos *et al.* 1967)

$$S^{(x)}(j_1 j_2; J_\mathrm{i} J_\mathrm{f}; I) = \langle \psi_{J_\mathrm{f}} \| [a^\dagger_{j_2} \times a_{j_1}]^{I(x)} \| \psi_{J_\mathrm{i}} \rangle, \tag{2}$$

in which the $a_{j_1}$ ($a^\dagger_{j_2}$) are annihilation (creation) operators for particles in the shells $j_1$ ($j_2$). These spectroscopic amplitudes are those multiparticle weights that determine reduced electric multipole probabilities to be

$$B(\mathrm{E}I; J_\mathrm{i} - J_\mathrm{f}) = \frac{1}{(2J_\mathrm{i}+1)(2I+1)} \left( \sum_{x j_1 j_2} e_x S^{(x)}(j_1 j_2; J_\mathrm{i} J_\mathrm{f}; I) \langle j_2 \| r^I Y_I \| j_1 \rangle \right)^2, \tag{3}$$

where $e_x$ is the appropriate effective charge. The remaining component of equation (1) is the two-body matrix element

$$M^{(x)}_{j_1 j_2 I} = \sum_{m_1 m_2 N} \langle J_\mathrm{i} I M_\mathrm{i} N \,|\, J_\mathrm{f} M_\mathrm{f} \rangle (-)^{j_1 - m_1} (2J_\mathrm{f}+1)^{-\frac{1}{2}} \langle j_1 j_2\, m_1 - m_2 \,|\, I - N \rangle$$
$$\times \langle \chi^{(-)}_\mathrm{f}(0)\, \phi_{j_2 m_2}(1) \,|\, t(01)\, \mathscr{A}_{01} + V_{\mathrm{cp}}(01) \,|\, \chi^{(+)}_\mathrm{i}(0)\, \phi_{j_1 m_1}(1) \rangle, \tag{4}$$

in which the $\chi^{(\pm)}$ are the relevant projectile wavefunctions (we use best-fit optical potential wavefunctions; Craig *et al.* 1966; Lewis *et al.* 1967) and the $\phi_{jm}$ are the single-proton (neutron) bound state wavefunctions (harmonic oscillator wave-

functions associated with oscillator energies of 14·4 and 13·7 MeV for $^{24}$Mg and $^{28}$Si respectively).

We have chosen to analyse 50 MeV data here in order that only a two-nucleon $t$ matrix $t(01)$ (the $\mathscr{A}_{01}$ being the antisymmetrization operator) and a core polarization correction $V_{cp}(01)$ are pertinent in the analyses. Core polarization corrections in reaction analyses are necessary whenever the spectroscopic model states used require core polarization contributions to explain observed electromagnetic transition rates. In the present analyses we follow the standard prescription (Love and Satchler 1970, 1971), using collective model form factors to generate the core polarization corrections to the (p, p′) transition amplitudes; whence the overall coupling strengths $y_2(Q)$ have a direct correlation to the effective charges that result from the analogous core polarization corrections to electromagnetic transition rates. This nexus is not universally valid (Amos *et al.* 1978) but should be true for the low excitation transitions in $N = Z$ nuclei.

Recent analyses of 20·3 MeV (**p**, p′) data (Lombard *et al.* 1978) and of 40 MeV (p, p′) data (Zwieglinski *et al.* 1978) from $^{24}$Mg used a more simplistic model than ours for core polarization, to wit a straight scaling of their chosen two-nucleon interaction strengths. In both of these analyses, the $2_1^+$ data were used to normalize those scalings against the known $B$(E2) value and the effective charges required by the nuclear structure calculations to fit that $B$(E2) value. In our case, the effective charges are deduced from the (p, p′) analyses without modification of either the strengths or the ranges of the two-nucleon interaction potentials of equation (5) below. Hence our analyses complement those of Lombard *et al.* and Zwieglinski *et al.* in that we confirm the equivalence (for the $2_1^+$ states) between effective charges required in inelastic scattering analyses and in electromagnetic transition rate calculations for a variety of models of the nuclear structure.

The two-nucleon $t$ matrix or 'valence' interaction was chosen to be the simple central even-state force (Wong and Wong 1967)

$$t(01) = -25\exp(-0{\cdot}275\,r^2)\,\delta_{S0}\,\delta_{T1} - 47\exp(-0{\cdot}3375\,r^2)\,\delta_{S1}\,\delta_{T0} \qquad (5)$$

that has been used with some success previously (Nesci and Amos 1977; Amos *et al.* 1978; Nesci *et al.* 1979). Tensor force and two-body spin–orbit force contributions have not been included because for $2^+$ state excitations, at least as far as differential cross sections are concerned, realistic forms of those forces only weakly influence predictions. Furthermore, computational time (and cost) is thereby kept within feasible bounds for all calculations. Nevertheless, this is a weak point of the analyses and the analysing power data will reflect any deficiency of this model $t$ matrix most clearly.

The spectroscopic amplitudes remain to be specified and, since we are concerned with isoscalar natural parity transitions in $N = Z$ nuclei, the proton and neutron values are identical. The superscript $x$ is therefore superfluous and so henceforth is omitted. Detailed derivations of calculational forms of the spectroscopic amplitudes have been published previously for the $SU(3)$ model spectroscopy (Nesci *et al.* 1979) and for the appropriate PHF model spectroscopy (Nesci and Amos 1977) and thus are not repeated herein. The values of these spectroscopic amplitudes are listed in Tables 1*a* and 1*b*: the former gives those pertinent to transition densities calculated from all the s–d basis models of spectroscopy, while the latter contains those obtained from the large basis models of nuclear structure that we have chosen.

**Table 1. Calculated spectroscopic amplitudes for different models**

The values listed are spectroscopic amplitudes calculated from shell model (SM), $SU(3)$ model, projected Hartree–Fock model (PHF) and Nilsson model (NM) spectroscopies. The results for the large basis models in (*b*) are divided into three groups *A*, *B* and *C* as described in the text

(*a*) $S(j_1 j_2; 0 J_f; J_f)$ *from s–d Basis Models*

| | $^{24}$Mg ($2_1^+$) | | $^{24}$Mg ($2_2^+$) | | $^{28}$Si ($2_1^+$) | | |
|---|---|---|---|---|---|---|---|
| $j_1 \to j_2$ | SM | $SU(3)$ | SM | $SU(3)$ | SM | $SU(3)$ | PHF |
| $d_5 \to d_5$ | 0·940 | 0·715 | 0·214 | 0·640 | 0·386 | 1·010 | 0·635 |
| $d_5 \to d_3$ | −0·457 | −0·357 | −0·382 | −0·320 | −0·258 | −0·505 | −0·695 |
| $d_5 \to s_1$ | 0·662 | 0·614 | 0·167 | −0·144 | 1·049 | 0·472 | 0·809 |
| $d_3 \to d_5$ | 0·467 | 0·357 | 0·141 | 0·320 | 0·227 | 0·505 | 0·611 |
| $d_3 \to d_3$ | 0·127 | 0·547 | 0·282 | 0·489 | 0·081 | 0·773 | 0·364 |
| $d_3 \to s_1$ | 0·254 | 0·501 | −0·076 | −0·012 | 0·087 | 0·386 | 0·083 |
| $s_1 \to d_5$ | 0·530 | 0·550 | 0·16 | −0·019 | 0·617 | 0·630 | 0·785 |
| $s_1 \to d_3$ | −0·258 | −0·449 | −0·048 | 0·015 | −0·196 | −0·514 | −0·258 |

(*b*) $S(j_1 j_2; 02; 2)$ *from Large Basis Models*

| (*A*) Within s–d | | | (*B*) Even parity | | | (*C*) Odd parity | | |
|---|---|---|---|---|---|---|---|---|
| | $^{24}$Mg | $^{28}$Si | | $^{24}$Mg | $^{28}$Si | | $^{24}$Mg | $^{28}$Si |
| $j_1 \to j_2$ | PHF[A] | NM | $j_1 \to j_2$ | PHF | NM | $j_1 \to j_2$ | PHF | NM |
| $0d_5 \to 0d_5$ | 0·831 | 0·612 | $0s_1 \to 0d_3$ | 0·123 | — | $0p_1 \to 0f_5$ | −0·217 | −0·106 |
| | (0·80) | | $0s_1 \to 0d_5$ | −0·164 | — | | | |
| $0d_5 \to 0d_3$ | −0·574 | −0·638 | $1s_1 \to 1d_5$ | 0·084 | −0·083 | $0p_3 \to 0f_5$ | 0·105 | — |
| | (−0·50) | | $1s_1 \to 1d_3$ | −0·013 | 0·072 | | | |
| $0d_5 \to 1s_1$ | 0·681 | 0·736 | $2s_1 \to 0d_5$ | 0·122 | — | $0p_3 \to 0f_7$ | −0·227 | −0·155 |
| | (0·81) | | $0d_3 \to 0s_1$ | −0·103 | — | | | |
| $0d_3 \to 0d_5$ | 0·595 | 0·576 | $0d_3 \to 0g_7$ | −0·04 | — | $0f_5 \to 0p_1$ | −0·168 | −0·085 |
| | (0·54) | | $0d_5 \to 0s_1$ | −0·209 | — | | | |
| $0d_3 \to 0d_3$ | −0·015 | 0·355 | $0d_5 \to 2s_1$ | 0·153 | — | $0f_7 \to 0p_3$ | −0·176 | −0·124 |
| | (−0·02) | | $0d_5 \to 1d_5$ | 0·142 | — | | | |
| $0d_3 \to 1s_1$ | 0·197 | 0·164 | $0d_5 \to 0g_9$ | −0·192 | −0·278 | $0f_7 \to 1p_3$ | −0·046 | — |
| | (0·22) | | $1d_5 \to 1s_1$ | 0·108 | −0·074 | | | |
| $1s_1 \to 0d_5$ | 0·543 | 0·737 | $1d_5 \to 0d_5$ | 0·140 | — | $1p_1 \to 0f_5$ | −0·048 | — |
| | (0·66) | | $1d_5 \to 0g_9$ | −0·032 | — | | | |
| $1s_1 \to 0d_3$ | −0·232 | −0·319 | $0g_9 \to 0d_5$ | −0·12 | −0·177 | $1p_3 \to 0f_7$ | −0·060 | — |
| | (−0·27) | | | | | | | |

[A] Values in parentheses are results obtained from an s–d basis PHF model for $^{24}$Mg.

It is evident from Table 1*a* that the $SU(3)$ model emphasizes all spectroscopic amplitudes, with d-orbit occupation in the spectroscopy being the most enhanced. In the case of $^{28}$Si, the PHF values tend to lie midway between the shell model and $SU(3)$ results, with notable differences from those of the (truncated) shell model values indicating a possible serious influence of the truncation shell model s–d basis space upon transition rates. This is in complete accord with the observation by Das Gupta and Harvey (1967) that the Hartree–Fock transition densities for $^{28}$Si reflect the role of the spin–orbit splitting which is ignored in an $SU(3)$ assignment but maximized in the shell model approach.

In Table 1*b* the large basis results (PHF for $^{24}$Mg and Nilsson model (NM) for $^{28}$Si) are divided into three groups. Group *A* contains those values associated with

single-nucleon transitions within the s–d shell; these may be compared directly with the values given in Table 1*a*. To complete the listing we include (in parentheses) in group *A* those values which were obtained when an s–d basis PHF model of spectroscopy for $^{24}$Mg was used (Braley and Ford 1969; Ford *et al.* 1971). Group *B* in Table 1*b* contains the spectroscopic amplitudes for all transitions between even parity single-particle states in which at least one of these states lies outside the s–d shell. In group *C* of Table 1*b* spectroscopic amplitudes for odd parity states (p–f) are given.

It is clear that the large basis calculations yield s–d shell spectroscopic amplitudes that are quite comparable with those of the smaller basis ones. Additionally, however, numerous other transition amplitudes and especially those between p and f orbits are not negligible. Indeed, the 'additional' transition components to those contained solely within the s–d shell will seriously influence predictions of transition rates (Zwieglinski *et al.* 1978); this is evident from the ensuing discussion of the results of our reaction analyses.

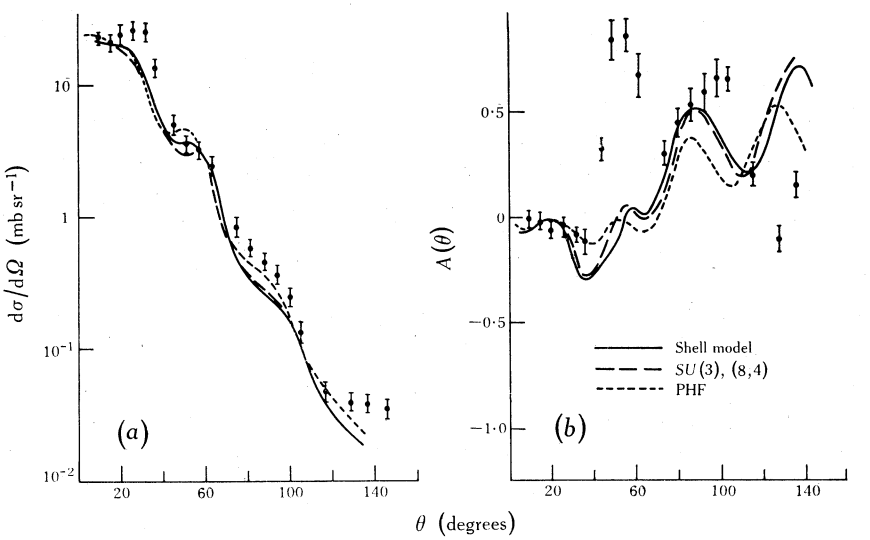


**Fig. 1.** Comparison of present DWA analyses with experimental data for (*a*) the differential cross section $d\sigma/d\Omega$ and (*b*) the analysing power $A(\theta)$, at a c.m. scattering angle $\theta$, from inelastic scattering of 49·5 MeV protons leading to the $2_1^+$ excitation (1·37 MeV) in $^{24}$Mg. The theoretical curves are from (full) s–d shell model, $SU(3)$ (8,4) model and (0s–0g) projected Hartree–Fock model (PHF) spectroscopies.

## 4. Results and Discussion

In Fig. 1, the results of our analyses of the differential cross section and analysing power from the inelastic scattering of 49·5 MeV protons leading to the $2_1^+$ (1·37 MeV) state in $^{24}$Mg are compared with experimental data. In these DWA analyses, those made using shell model (solid curves) and $SU(3)$ model (long-dashed curves) spectroscopies included core polarization corrections to the transition interaction. On the other hand, the analyses made using the large basis PHF spectroscopy (short-dashed curves) had no such core polarization corrections since that spectroscopy required

no polarization charge to match the observed $B$(E2) value for the de-excitation (to ground) of the $2_1^+$ state. It is evident from Fig. 1*a* that all three model spectroscopies predict essentially the same differential cross section and one that is in good agreement with the measured data.

Since the PHF model required no polarization charge, the inelastic scattering DWA calculations had no core polarization corrections to the effective two-nucleon transition interaction, thereby being unencumbered by the uncertainties and ambiguities introduced by use of phenomenological collective model form factors. With no other data, therefore, one would be satisfied that core polarization effects had been accounted for by the large basis spectroscopy.

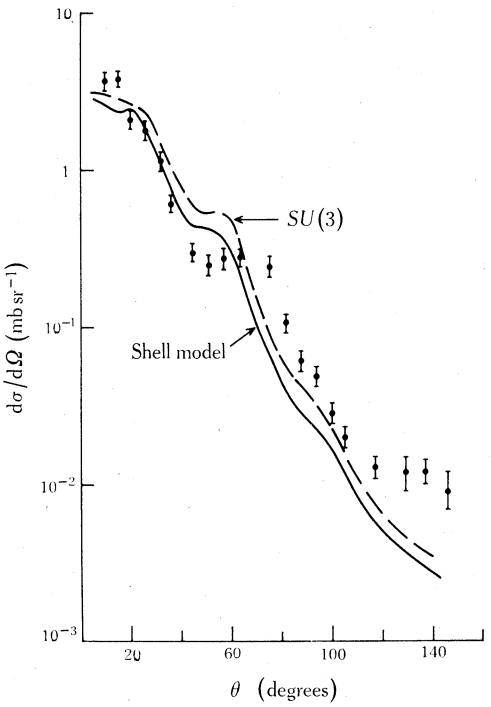


**Fig. 2.** Comparison of DWA analyses with experimental data for the differential cross section from inelastic scattering of 49·5 MeV protons leading to the $2_2^+$ excitation (4·24 MeV) in $^{24}$Mg. The theoretical curves are from (full) s–d shell model and $SU(3)$ model spectroscopies.

None of the reaction calculations however, reproduce the observed analysing power data (Fig. 1*b*). Since the PHF result is observably different from that of either the shell model or the $SU(3)$ model, and is also more dissimilar to the data structure than the other two, it is tempting to attribute all the discrepancies to inadequacies in the character and specifications of the 'valence' interaction ($t$ matrix). But the major anomaly is located at $\theta = 60°$ in the centre of mass system, at which scattering angle the differential cross section is large (and well reproduced by our model calculations), and other studies have shown that reasonable tensor and two-body spin–orbit effects in forward angle $2_1^+$ cross sections are not large. Thus it is not certain that improvements to the $t$ matrix will explain the observed analysing power mismatch. This conclusion is supported by the observation of just such an anomaly between previous analyses and analysing power data from a variety of nuclei (Kolata and Galonsky 1969; Greaves *et al.* 1972; Nesci and Amos 1977;

Lombard *et al.* 1978), such analyses using a variety of prescriptions for the reaction mechanism. In any event, these results suggest that the core polarization corrections are due, in large measure, to omissions of the neighbouring shells from the usual model spectroscopies. Furthermore, the emphasis of the $SU(3)$ model spectroscopy to transitions involving the $d_{3/2}$ and $s_{1/2}$ orbits over that of the full shell model (as seen from the spectroscopic amplitudes in Table 1*a*) has no great consequence for the resulting transition strengths and distributions. However, in this regard the

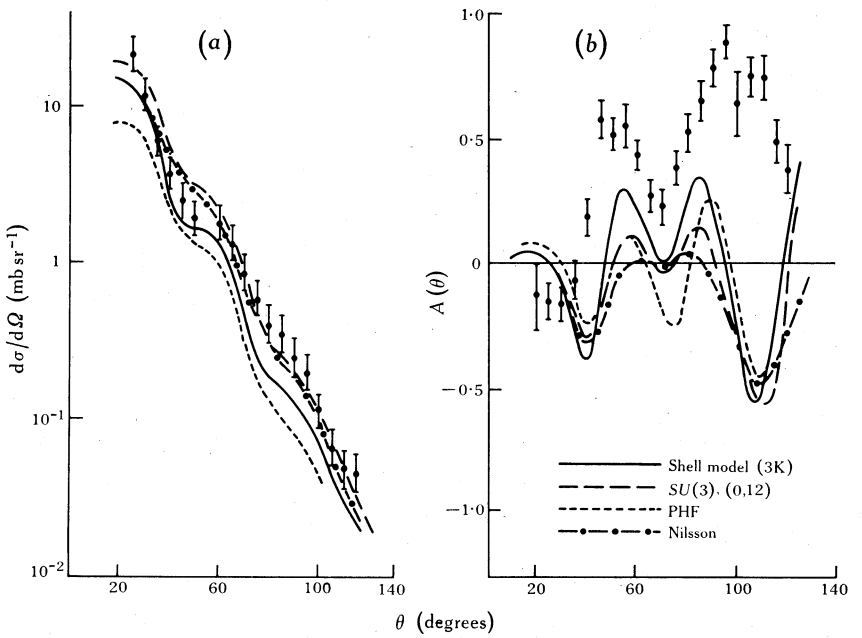


**Fig. 3.** Comparison of DWA analyses with experimental data for (*a*) the differential cross section and (*b*) the analysing power from inelastic scattering of 49·5 MeV protons leading to the $2_1^+$ excitation (1·78 MeV) in $^{28}$Si. The theoretical curves are from a truncated s–d shell model, an $SU(3)$ (0, 12) model, an s–d PHF model, and a Nilsson model in which the deformed potential was adjusted to give states that required no effective charge to account for electromagnetic transitions between them.

cross-band transition, to the $2_2^+$ state, should be more instructive, since the $SU(3)$ and shell model spectroscopies yield different transition densities. Previously such differences led to quite dramatic effects in predictions of inelastic proton scattering transitions to the $3^+$ member of the $K = 2$ band (Nesci *et al.* 1979); but both models failed to reproduce the observed data. Such dramatic variation is not seen in the present analyses of the $2_2^+$ transition data, however, and, as shown in Fig. 2, when core polarization corrections corresponding to polarization charges of $0{\cdot}5e$ and $0{\cdot}4e$ for the shell model and $SU(3)$ model calculations respectively are incorporated in the reaction analyses, the resulting predictions are in reasonable agreement with one another and also with the data. It remains to be seen whether or not the distinct discrepancies between these predictions and the data are as significant and useful in criticizing spectroscopy as the very large ones previously found from the analyses of the $3^+$ excitations. Overall, it seems clear that neither the full s–d basis shell

model nor its approximant, the $SU(3)$ model that stresses collectivity, is adequate to describe the $K = 2$ band excitations in $^{24}$Mg by inelastic scattering, at least in a first-order reaction theory.

The $^{28}$Si data and the results of our analyses are displayed in Fig. 3. The shell model (truncated s–d basis), $SU(3)$ (0, 12) representation model and s–d basis PHF results all include core polarization corrections, the coupling constants of which correspond to polarization charges of $0{\cdot}63\,e$, $0{\cdot}21\,e$ and $0{\cdot}32\,e$ respectively. Only the Nilsson model result, by the construction of this model spectroscopy, has no core polarization corrections.

Save for the PHF and shell model results being slightly too weak, all spectroscopies result in DWA predictions that are in good agreement with the differential cross section data in Fig. 3*a*. However, no calculation reproduces the large positive analysing power measurements (Fig. 3*b*); albeit that the gross structural features of the data are seen in most of the predictions. The purely particle interaction (no core polarization) results of the Nilsson model are the least like the data. Thus the mismatch between the analysing power data and the predictions would again appear to be evidence of an incomplete description of the reaction mechanism rather than flaws in the spectroscopy. Indeed, the recent analyses of inelastic proton scattering data by Lombard *et al.* (1978) and Zwieglinski *et al.* (1978) suggest that a coupled channels approach will be required before such discrepancies may be resolved, for quite good results were obtained by using an asymmetric rotational model for the interaction form factors in coupled channels calculations. Even so, a number of problems remained, not the least of which were poor fits to $K = 2$ band state excitation data in both magnitude and shape, and the need to use a large spin–orbit potential deformation to get fits to the analysing power data for ground state band transitions. However, with 20·3 MeV incident energy, higher order processes in which the giant resonances of $^{24}$Mg act as doorway states (Geramb *et al.* 1975) are significant, and this is evident by the tendency of the analysing powers from weak transitions to have a symmetry about 90° in the centre of mass system, by the large angle enhancement in weak transitions and by the larger scale factors required in the 20·3 MeV analysis (Lombard *et al.* 1978) when compared with those in the 40 MeV analysis (Zwieglinski *et al.* 1978).

Despite the above problems, the introduction of channel coupling may help to resolve the discrepancies between the present DWA predictions and the experimental data. However, in view of the distinctive effects in first-order analyses of the finite range of the two-nucleon $t$ matrix and of antisymmetrization, the pertinent coupled channels calculation is yet to be constructed. Antisymmetrization of the total wavefunctions, in particular, should have a drastic effect upon predictions of analysing powers since, even in our first-order theory, its inclusion causes substantial changes to data predictions (Amos and Smith 1974).

## References

Akiyama, Y., Arima, A., and Sebe, T. (1969). *Nucl. Phys.* A **138**, 273.
Amos, K., Faessler, A., Morrison, I., Smith, R., and Muether, H. (1978). *Nucl. Phys.* A **304**, 191.
Amos, K., Madsen, V. A., and McCarthy, I. E. (1967). *Nucl. Phys.* A **94**, 103.
Amos, K., and Smith, R. (1974). *Nucl. Phys.* A **226**, 519.
Braley, R. C., and Ford, W. F. (1969). *Phys. Rev.* **182**, 1174.
Chung, W., and Wildenthal, B. H. (1978). Michigan State Univ. Preprint No. MSUCL–218.

Craig, R. M., Dore, J. C., Greenlees, G. W., Lowe, J., and Watson, D. L. (1966). *Nucl. Phys.* A **83**, 493.
Das Gupta, S., and Harvey, M. (1967). *Nucl. Phys.* A **94**, 602.
Draayer, J. P., and Akiyama, Y. (1973). *J. Math. Phys.* (*Cambridge, Mass.*) **12**, 1904.
Ford, W. C., Braley, R. C., and Bar-Touv, J. (1971). *Phys. Rev.* C **4**, 2099.
Geramb, H. V., *et al.* (1975). *Phys. Rev.* C **12**, 1697.
Greaves, P. D., Hnidzo, V., Lowe, J., and Karban, O. (1972). *Nucl. Phys.* A **179**, 1.
Kolata, J. J., and Galonsky, A. (1969). *Phys. Rev.* **182**, 1073.
Lewis, V. E., Burge, E. L., Rush, A. A., Smith, D. A., and Ganguly, N. J. (1967). *Nucl. Phys.* A **101**, 598.
Lombard, R. M., Escudié, J. L., and Soyeur, M. (1978). *Phys. Rev.* C **18**, 42.
Love, W. G., and Satchler, G. R. (1970). *Nucl. Phys.* A **159**, 1.
Love, W. G., and Satchler, G. R. (1971). *Nucl. Phys.* A **172**, 449.
Nesci, P., and Amos, K. (1977). *Nucl. Phys.* A **284**, 239.
Nesci, P., Morrison, I., and Amos, K. (1979). *J. Phys.* G **5**, 387.
Rush, A. A., Burge, E. L., Lewis, V. E., Smith, D. A., and Ganguly, N. K. (1967). *Nucl. Phys.* A **104**, 340.
Schwalm, D., Warburton, E. K., and Olness, J. W. (1977). *Nucl. Phys.* A **234**, 425.
Strottman, D. (1972). *Phys. Lett.* B **39**, 457.
Whitehead, R., Watt, A., Cole, B., and Morrison, I. (1977). *Adv. Nucl. Phys.* **9**, 123.
Wildenthal, B. H., and McGrory, J. B. (1973). *Phys. Rev.* C **7**, 713.
Wong, C. W., and Wong, C. Y. (1967). *Nucl. Phys.* A **91**, 433.
Zwieglinski, B., Crawley, G. M., Chung, W., Hann, H., and Nolen, J. A. (1978). *Phys. Rev.* C **18**, 1228.

Manuscript received 19 November 1979, accepted 20 February 1980